

## **REMARKS**

Claims 1-8, 10, and 33-35 are pending in the application; Claims 1 and 10 are amended; Claims 1-8, 10, and 33-35 stand rejected.

## **DOUBLE PATENTING**

Claims 1-8, 10, and 33-35 are rejected on the grounds of nonstatutory obviousness type double patenting. Applicant submits that a terminal disclaimer will be filed when an indication of allowable claims is received.

## **REJECTION OF CLAIMS UNDER 35 U.S.C. §103(a)**

Claims 1-7 and 33-35 are rejected 35 USC 103(a) as allegedly obvious in view of Castillo, Hornbeck and Grainger.

The office action sets out that Castillo teaches an assay akin to an ELISA where SGAGs (perlecan) is immobilized on a titer well plate and then A $\beta$  is added in a 1:1 ratio. Castillo does not teach the step of air drying the SGAGs on the plate.

The office action then considers the disclosure of Hornbeck which teaches six different permutations of immunoassays used to detect and quantify the amount of specific reagent in solution. As noted in the office action, Hornbeck does not explicitly teach the step of air-drying or SGAGs and A $\beta$  as recited in the claims.

Finally the office action characterizes the disclosures of Grainger who teaches an ELISA to measure TGF- $\beta$  where the capture antibody is air dried on ELISA plates.

The office action then presents rationale which would allegedly explain why the skilled person would be motivated to combine the step of air drying as taught by Grainger with the method of Castillo. It is stated that such motivation would result in an accurate and reliable ELISA-type assay for quantitating the amount of A $\beta$  in a sample. Examiner further states that allowing the product to air dry would be advantageous as it would assure that all of the first reagent would be immobilized onto the substrate. And that incorporating a drying step into the method of Castillo would ensure that more perlecan was immobilized onto the substrate which would thereby allow a greater range of detection.

### The Legal Standard

A finding of obviousness requires that "the differences between the subject matter sought to be patented and the prior art are such that the subject matter as a whole would have been obvious at the time the invention was made to a person having ordinary skill in the art to which said subject matter pertains." 35 U.S.C. §103(a). In its recent decision addressing the issue of obviousness, *KSR International Co. v. Teleflex Inc.*, 127 S.Ct. at 1741, 82 USPQ2d 1396 (2007), the Supreme Court stated that it is "important to identify a reason that would have prompted a person of ordinary skill in the relevant field to combine the elements in the way the claimed new invention does..... because inventions in most, if not all, instances rely upon building blocks long since uncovered, and claimed discoveries almost of necessity will be combinations of what, in some sense, is already known." See also USPTO Examination Guidelines for Determining Obviousness Under 35 U.S.C. 103 in View of the Supreme Court Decision in *KSR International Co. v. Teleflex Inc.*, 72 Fed. Reg. 57,526, 57,528 (Oct. 10, 2007) ("it remains necessary to identify the reason why a person of ordinary skill in the art would have combined the prior art elements in the manner claimed.").

Thus, consistent with the principles enunciated in *KSR*, obviousness can be established by showing a suggestion or motivation, either in the references themselves or in the knowledge generally available to one of ordinary skill in the art, to modify the reference and to carry out the modification with a reasonable expectation of success, viewed in light of the prior art. Both the suggestion and the reasonable expectation of success must both be found in the prior art and *not* be based on the applicant's disclosure. *In re Dow Chemical Co.*, 837 F.2d 469, 5 USPQ2d 1529 (Fed. Cir. 1988).

Applicant submits that a *prima facie* case of obviousness has not been established because the reasons stated to motivate the person ordinarily skilled in the art to combine the references are not without potential drawbacks which would require further significant experimentation and thus diminish the expectation of success to below the "reasonable" threshold.

As stated by the Examiner, the step of air drying combined with the ELISA-type assay of Castillo would provide an "accurate and reliable ELISA-type assay for quantitating the amount of A $\beta$  in a sample". Why would the ordinarily skilled person, already in possession of an ELISA-type assay (as described by Castillo) as well as the

PATENT

highly accurate and reliable regular types of ELISA's (as described in Hornbeck) which are perfectly suited to quantitating the amount of A $\beta$  in a sample, seek to add further steps to the already complicated method of Castillo when nothing further in terms of accuracy or reliability would be obtained by the modification?

The Examiner further alleges that allowing the product to air dry would be advantageous as it would assure that all of the first reagent would be immobilized onto the substrate. In support of this allegation the Examiner notes that Castillo teaches that only about 20% of perlecan immobilized on the microtitre well and thus incorporating a drying step into the method of Castillo would ensure that *more perlecan was immobilized onto the substrate which would thereby allow a greater range of detection.*

With respect to air drying, Applicant submits that the person ordinarily skilled in the art would appreciate that the plastic surface of the well of the ELISA plate has a finite saturation level for the first reagent and that the amount of reagent bound to the substrate is a function of hydrophobic interactions between the reagent and the plastic surface. Drying the reagent onto the plate may not unequivocally alter the total amount of perlecan bound since dried but unbound perlecan would be removed by subsequent washes. The person ordinarily skilled in the art would further appreciate that binding density of the first reagent, if too high, may interfere with subsequent antibody binding due to steric hindrance and that stacking or layering the first reagent on the plate may also affect the accuracy of the assay.

The skilled person will also appreciate that there is potential for air drying to cause concentration dependent effects since it will increase the concentration of protein in solution, the concentration of salts in the solution as well as decrease the pH [Please see attached articles in the appendix entitled "Maintaining the Stability of dry and liquid protein reagents can require significant experimentation during the product development phase of a new immunoassay" and Lyophilization-induced reversible changes in secondary structure of proteins"]. The concentration effect caused by air drying could therefore change protein/proteoglycan binding to plate or more importantly alter the subsequent binding of the proteoglycan to A $\beta$ . This modification could therefore destroy the function of Castillo which was to study the binding affinity between perlecan and A $\beta$ . Perlecan is not akin to the well characterized antibody which is the

PATENT

typical first reagent in an ELISA, but a proteoglycan which is a large and complex molecule with a core protein linked by a trisaccharide to a glycosaminoglycan (linear negatively charged carbohydrate polymer) on which drying could have unforeseen and unanticipated effects.

For these reasons Applicant submits that the proposed modification is not without potential pitfalls and hence the expectation of success is diminished and the function of Castillo might also be destroyed. In view of the discussion above and the claim amendments, applicant respectfully requests that the rejection be withdrawn.

Claims 1-8 and 33-35 are rejected 35 USC 103(a) as allegedly obvious in view of Castillo, Hornbeck, Grainger and further in view of Cross.

Claims 1-8 and 33-35 are rejected 35 USC 103(a) as allegedly obvious in view of Castillo, Hornbeck, Grainger, Cross and further in view of Roach.

Since these further 103(a) rejections rely on the primary rejection in view of Castillo, Hornbeck, and Grainger as set out above, applicant respectfully requests that these rejections also be withdrawn.

Applicant believes it has responded fully to all of the Examiner's concerns. If the Examiner has any further concerns, Applicant urges a call to Rebecca Eagen at (425) 823-0400 extension 39.

Respectfully submitted



REBECCA EAGEN  
Reg. No. L0386

PROTEOTECH, INC.  
12040 115<sup>TH</sup> AVE NE  
KIRKLAND, WA 98034

PATENT

**APPENDIX**

[Print this Page](#)[IVD Technology Magazine](#)[IVDT Article Index](#)

## Stability issues for protein-based in vitro diagnostic products

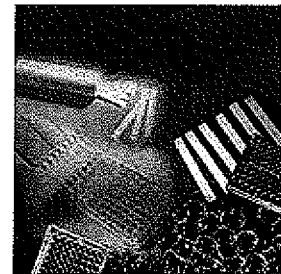
Patrick E. Guire

***Maintaining the stability of dry and liquid protein reagents can require significant experimentation during the product development phase of a new immunoassay.***

Diagnostic immunoassay products are based on proteins, a class of biochemical macromolecules named after the Greek mythical fast-change artist, Proteus. Like their namesake, proteins have the ability to change their shape, which can lead to loss of activity. The specific-binding and catalytic functions of protein reagents, such as antibodies, lectins, and enzymes, are quite sensitive to the potentially detrimental effects of preparation, storage, and handling.

This article discusses the various issues in protein stability that are of concern to the manufacturers of IVD products. These issues may be broken down into those concerning reagents that will be dried and those concerning reagents kept in solution.

Drying and/or freezing steps have the potential to severely denature proteins unless the proteins are properly protected. The correct drying methods and storage conditions are vital to the shelf life of dried components. Liquid stabilization is affected by a larger number of variables. Temperature, microbial contamination, and pH level or buffer can all affect stability.



Additionally, this article will discuss why performance problems should not be automatically attributed to stability issues. Factors in the production protocol may be the culprits.

### The Nature of Protein

Proteins are flexible polymeric molecules with functional three-dimensional catalytic or binding sites.<sup>1</sup> The spatial arrangement of amino acids in the catalytic and/or binding site is dependent upon the interaction of these amino acids with one another, the solvent, and solute molecules.<sup>2-4</sup>

Protein molecules comprise both hydrophilic and hydrophobic amino acids. This composition results in the protein's spontaneous folding in aqueous solution, with the more hydrophobic amino acids clustered in "dry pockets" inside a globular molecule and the more polar amino acids concentrated on the hydrated exterior.<sup>5,6</sup>

Other crosslinking interaction forces include electrostatic, H-bond, van der Waals, chelation, and covalent (e.g., disulfide bonds). Several of these interaction forces are strongly sensitive to the effects of phase changes (freezing and drying).

### Problems with Dry Stabilization

While most specific-binding proteins function in the aqueous state in nature, the dry or frozen state is much preferred for stable storage. In these relatively immobile states, the frequency of collision with harmful cosolutes, such as proteases or oxidants, is immensely reduced. However, removal of solvent from protein molecules through drying—or through other phase changes such as precipitation and freezing—puts stress on the functional conformation of proteins. These phase changes can expose the hydrophobic amino acids normally buried within the molecule. Such exposure increases the proteins' association with other molecules and with hydrophobic surfaces, resulting in denaturation of the protein molecules.

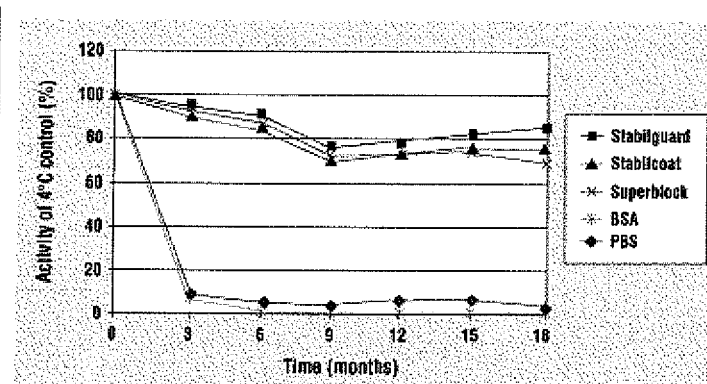


**Figure 1. Monoclonal antibody room temperature stability study.**

Drying steps include air-drying or freeze-drying of, for example, conjugates in vials or antibody-coated plastic or membrane material. One hazard to avoid is unintentional drying between steps, which can result from working with too large a batch of coated product (plates or tubes) at one time or working in an extremely dry environment.

Inclusion of compatible solutes in the drying solution to prevent denaturation is an effective approach to stabilizing proteins for storage. These solutes typically contain hydrophilic groups, which stabilize the functional conformation of the protein molecules by burying the hydrophobic amino acids within. Therefore, it is very important to apply a stabilizing solution before the removal of solvent has promoted protein-protein and especially protein-surface interactions.

#### Use of Commercial Stabilizers

Commercial stabilizers are available to optimize shelf life. In one experiment, 96-well polystyrene plates (Immulon 2; Dynex Technologies Inc.; Chantilly, VA) were coated with monoclonal or polyclonal antibodies. They were then stabilized with one of the following: Stabilguard biomolecule stabilizer (SurModics Inc.; Eden Prairie, MN), Stabilcoat immunoassay stabilizer (SurModics Inc.), Superblock blocking buffer (Pierce Chemical Co.; Rockford, IL), or bovine serum albumin (BSA). Phosphate-buffered saline (PBS) was included as a negative control. The plates were then dried and stored in sealed foil pouches with desiccant. After storage at room temperature, the monoclonal plates were subjected to a sandwich enzyme immunoassay (EIA). A direct-binding assay with horseradish peroxidase (HRP) as the antigen was used for the polyclonal plates.

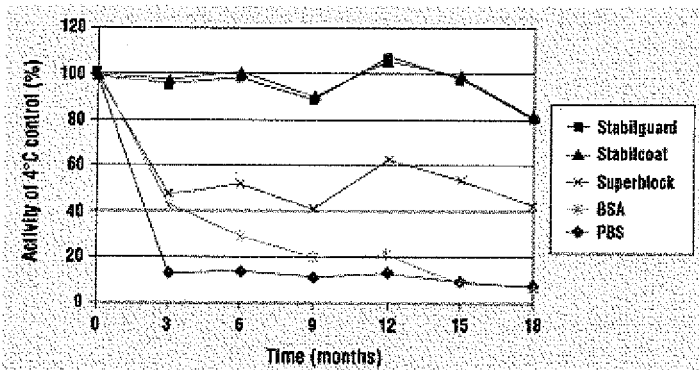


**Figure 2. Polyclonal antibody room temperature stability study.**

After 18 months storage at room temperature, all the samples, except those with BSA as the stabilizing agent, had good activity recovery in the range of 70 to 85% (see Figure 1). More pronounced differences were seen with the polyclonal antibody (see Figure 2). However, the 50% activity loss with Superblock seems to have occurred during the drying step, leaving an activity level fairly stable to storage thereafter. The fact that this activity loss was seen with the polyclonal but not the monoclonal antibody illustrates the possibility that testing multiple products may be necessary to find the stabilizer that works best for each system.

#### Effect of Drying Methods

Both drying methods and storage conditions are critical to maintaining stability. Membrane applications generally require very fast drying or lyophilization to retain optimum performance and activity. For coated plates, tubes, or beads, drying rapidly is not as important as ensuring that the components are completely dry. All dried products need to be stored in an airtight container with desiccant for maximum shelf life.

Following are data from a study of the effect of different drying methods on antibody activity after storage at room temperature for 6 and 12 months (see Figure 3). For the comparison of the effects of drying methods, 96-

well plates were incubated with monoclonal antirabbit antibody and washed. Stabilguard biomolecule stabilizer and Superblock blocking buffer were added to separate sections of the same plate and, after incubation, removed by aspiration. The plates were then dried by the following commonly available methods:

Four hours in a dry room atmosphere (16% relative humidity) at room temperature (20–24°C).

Four hours inside a sealed plastic bag containing desiccant (23% relative humidity) at room temperature.

Two hours in a drying oven (26% relative humidity) at 37°C.

For a negative control, plates were stored wet for 90 minutes in a sealed foil pouch without desiccant at room temperature.

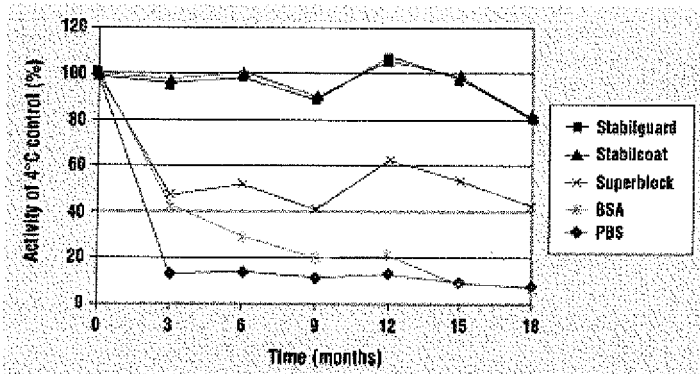


**Figure 3.** Percent of activity retained by monoclonal antirabbit antibody samples prepared using either Stabilguard or Superblock, dried using one of four techniques (including an undried control), and stored at room temperature for 6 and 12 months.

The plates were then placed in sealed foil pouches with desiccant and stored for long-term stability assessment at room temperature. The activity recovery was measured in a sandwich EIA using rabbit antibody as the analyte and goat antirabbit antibody-HRP as the second antibody. The standard or 100% activity value was that found with plates freshly prepared (i.e., not dried) at the time of the assay.

While the differences among the methods were not profound, the drying room method consistently gave the best results. Had the long-term storage pouch not contained desiccant, greater activity loss of the negative control would most likely have been observed.

#### Problems with Solution Stabilization

While aqueous solution is the natural functioning state for antibodies, enzymes, and other diagnostic proteins, this is not their state of greatest stability. Numerous factors may affect the functional activity of proteins while they are in solution:

The protein molecules become more flexible and prone to conformational changes.

The frequency of collision with other molecules and/or the container surface increases.

The possibility of microbial contamination increases.

Sensitivity to elevated temperatures and low protein concentrations is heightened.

The proteins become more susceptible to oxidation.

As a general rule, the dissolved protein molecule is most stable at lower temperatures and higher protein concentrations. At just above freezing temperature, the protein molecule has less of the kinetic energy required to "escape" its minimum energy functional conformation(s). At higher protein concentrations (the microgram per milliliter range or higher), a lower fraction of the total protein activity is lost through the adsorption of the protein molecules to the container surface, the dissociation of multisubunit enzymes, and inactivation by low levels of contaminating solutes such as oxidants, hydrolytic enzymes, and microorganisms.

#### The Importance of Proper pH Level

The functional conformations of protein molecules are stabilized by interactions with ionic cosolutes, through electrostatic and/or chelate bridging within the molecule.<sup>7,8</sup> The sensitivity of catalytic proteins (enzymes) to pH or hydrogen ion concentration is especially well known, leading to the almost universal use of buffer cosolutes to maintain the desired pH of the enzyme solution. Perhaps less widely recognized is the sensitivity of the enzyme to the chemical character of the buffer ion.

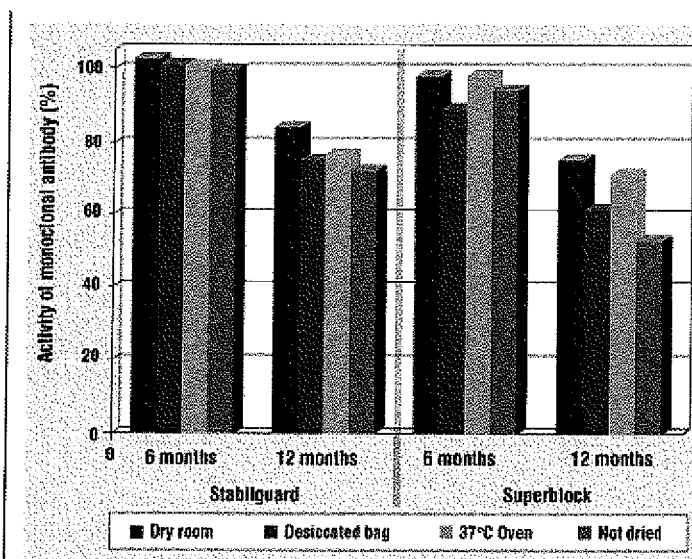


**Figure 4. Effect of pH on stability.** Solutions tested were HEPES (a), citrate (b), MOPS (c), glycine (d), Tris (e), and saline (f), all mixed 1:1 in Stabilzyme Select conjugate stabilizer and stored at 37°C. Each graph shows the percentage of activity retained by the test solution compared to a control stored at 4°C.

Following are data from a stability study of an enzyme-antibody conjugate in aqueous solution containing Stabilzyme Select conjugate stabilizer (SurModics Inc.) in various buffers and saline at different pH values. The data were obtained with a direct EIA using goat antirabbit antibody-HRP conjugate on freshly prepared rabbit antibody plates.

Five different pH values were tested. Some of the pH values tested were notably outside the useful range for a specific buffer, but all were included to directly compare the effect of different buffer molecules. The five buffers examined were:

citrate  
glycine  
N-(2-hydroxyethyl)piperazine-N'-(2-ethanesulfonic acid) (HEPES)  
3-(N-morpholino)propanesulfonic acid (MOPS)  
Trizma Base (tris[hydroxymethyl]-aminomethane) (Tris).

The sixth solution tested was isotonic saline.

The buffers were prepared at a 0.1-mole concentration, divided, and adjusted to the five different pH levels. They and the saline were then mixed 1:1 with a preparation of buffer-free Stabilzyme Select. The pH was tested again and adjusted if necessary. The conjugate was diluted 1:20,000 in these solutions before storage. The conjugate solutions were stored at 4°C and 37°C for 30 days.

The solutions were equilibrated to room temperature before testing of EIA activity. The pH was also tested at each time point. Most solutions remained within 0.2 units of the original pH. However, at 37°C, citrate, glycine, and saline showed a greater decrease in pH over time when the original pH levels were higher than 7.0. Retained activity values from conjugate solutions stored at 37°C are expressed as the percentage of the respective activities at 4°C (see Figure 4).

The recovered EIA activity of the antibody-HRP conjugate differs significantly among solutions containing different buffer ions as well as among solutions with different pH levels for each buffer. HEPES provided useful stability only at the lowest pH (6.0) and citrate at none of the pH values. The citrate's pH dependence was low; however, poor stability might result from its competition, by virtue of its chelating activity, with the conjugate for required polyvalent cations. The other solutions effectively stabilized the conjugate at activity recovery rates of 75% or better over 30 days, although not at all pH levels.

MOPS exhibited highest retained activity at pH levels between 6 and 7. Glycine, Tris, and saline performed best at pH levels between 6 and 7.7. Surprisingly, saline in Stabilzyme Select provided stability as good as that of all the buffers at pH 6 to 7.7 and better at pH 8.5. This study demonstrates the importance of selecting both the appropriate buffer and the optimal pH for an assay system.

#### Additional Sources of Stability Problems

Protein sources, purification methods, and conjugation chemistries can affect the activity and stability of protein reagents. For example, the source of alkaline phosphatase can have a profound effect on conjugate stability. Separation of the desired protein(s) from active harmful enzymes (e.g., hydrolases, oxidases) in the source material is of major importance to storage stability in solution. The removal or inactivation of these contaminating enzymes, and the viable microbial cells that produce them, is necessary for solution stability.

Numerous chemical procedures have been demonstrated for forming covalent bonds between the enzyme and the antibody molecule in conjugate preparation. Some of the procedures are much less destabilizing for certain enzyme and antibody combinations than are others. If an enzyme conjugate is losing EIA activity but retaining enzyme activity, electing an alternative conjugation chemistry may resolve the stability issue.

#### Other Performance Issues

Occasionally, issues that are assumed to be stability problems are actually deficiencies caused by other variables. The problem may be something as obvious as a dilution error. Manufacturers must reject container materials that could potentially adsorb and/or inactivate proteins, such as raw polystyrene, polysulfone, polycarbonate, or glass. Preferable container materials would be polyethylene or polypropylene. Colored enzymes and other protein solutions containing oxidative metal ions should not be exposed to light. Poor control of temperature for both the storage and the enzyme assay stages can be a significant cause of variability. Careless timing of the enzyme activity measurement stage of the assay can also be a factor.<sup>9</sup> As mentioned earlier, allowing coated wells, tubes, or beads to dry between steps can also cause variability.

#### Conclusion

Antibodies, enzymes, and other water-soluble proteins represent a major portion of the materials used in diagnostic immunoassays. To safeguard the shelf life and accuracy of these diagnostic tests, the proteins must be kept stable and viable.

Drying has the potential to severely denature proteins unless they are properly protected. The manner in which the protein-coated components are dried and stored is also very important. Storage in an airtight, desiccated environment helps to ensure long-term stability.

With liquid storage, the number of potentially destructive variables increases. Simple aspects, such as changes in pH level or buffer, can make significant differences in the stability of proteins in solution.

Liquid stabilization methods effective for one product may not be effective for another. Commercially available stabilizers address specific stabilization concerns. Testing a number of these products may identify a highly effective stabilizer for a specific need.

Other factors in the production protocol may affect performance. These factors include source of materials, dilution and timing errors, inappropriate temperature and humidity, exposure to light, and container materials. Finally, elementary as it may seem, when using a commercially produced stabilizing agent, one must be sure to follow package directions.

#### References

1. A Sali, E Shakhnovich, and Martin Karplus, "How Does a Protein Fold?" *Nature* 369 (1994): 248–251.
2. IM Klotz, "Protein Conformation: Autoplastic and Alloplastic Effects," *Archives of Biochemistry and Biophysics* 116 (1966): 92–96.
3. T Asakura, K Adachi, and E Schwartz, "Stabilizing Effect of Various Organic Solvents on Protein," *Journal of Biological Chemistry* 253 (1978): 6423–6425.
4. VP Torchilin, "Enzyme Stabilization without Carriers," *Enzyme and Microbiological Technology* 1 (1979): 74–82.
5. MI Kanehisa and TY Tsong, "Local Hydrophobicity Stabilizes Secondary Structures in Proteins," *Biopolymers* 19 (1980): 1617–1628.
6. SK Burley and GA Petsko, "Aromatic-Aromatic Interaction: A Mechanism of Protein Structure Stabilization," *Science* 229 (1985): 23–28.
7. FH Arnold and J-H Zhang, "Metal-Mediated Protein Stabilization," *Trends in Biotechnology* 12 (1994): 189–192.
8. EC Dawson, JDH Homan, and BK VanWeemen, Stabilization of Peroxidase, U.S. Pat. 4,228,240, October 14, 1980.
9. HU Bergmeyer ed., *Methods of Enzymatic Analysis*, 3rd ed. (Deerfield Beach, FL: Verlag Chemie, 1983).

**Patrick E. Guire, PhD, is senior vice president, chief scientific officer, and a founder of SurModics Inc. (Eden Prairie, MN).**

© Canon Communications LLC 2008

This contribution is part of the special series of Inaugural Articles by members of the National Academy of Sciences elected on April 25, 1995.

## Lyophilization-induced reversible changes in the secondary structure of proteins

(Fourier-transform infrared spectroscopy/dehydration/ $\alpha$ -helix/ $\beta$ -sheet/solid state)

KAI GRIEBENOW AND ALEXANDER M. KLIBANOV\*

Department of Chemistry, Massachusetts Institute of Technology, Cambridge, MA 02139

Contributed by Alexander M. Klibanov, August 28, 1995

**ABSTRACT** Changes in the secondary structure of some dozen different proteins upon lyophilization of their aqueous solutions have been investigated by means of Fourier-transform infrared spectroscopy in the amide III band region. Dehydration markedly (but reversibly) alters the secondary structure of all the proteins studied, as revealed by both the quantitative analysis of the second derivative spectra and the Gaussian curve fitting of the original infrared spectra. Lyophilization substantially increases the  $\beta$ -sheet content and lowers the  $\alpha$ -helix content of all proteins. In all but one case, proteins become more ordered upon lyophilization.

Consider the common laboratory and bioindustrial process of lyophilization or freeze-drying of aqueous solutions of proteins. Suppose that this lyophilization is carried out such that no irreversible damage to the protein ensues—i.e., when the lyophilized protein is redissolved in water, it exhibits the same properties as prior to lyophilization. The question still remains whether the protein structure in the lyophilized form is native or whether the lyophilization has resulted in reversible protein denaturation. Apart from its biochemical interest, the answer has important biotechnological implications. For example, proteins that have been lyophilized (which is how research and pharmaceutical protein preparations are usually stored) undergo moisture-triggered aggregation (1). To understand the mechanism of this undesirable phenomenon and to develop rational strategies for its prevention, structural information on proteins in the solid—e.g., lyophilized—form is needed. In addition, lyophilized enzymes suspended in organic solvents have proven to be useful synthetic catalysts (2); enzyme structural data should help maximize their performance.

The issue of protein conformation in the lyophilized form is controversial. For example, the results of Fourier-transform infrared (FTIR) spectroscopic investigations of hen egg-white lysozyme were interpreted to indicate that lysozyme structure in either aqueous solution or the lyophilized state is the same (3–6). This conclusion was supported by some hydrogen isotope-exchange studies (6, 7) but contradicted by others (8). Raman (9–11) and solid-state NMR (12) studies have suggested significant (reversible) structural changes occurring in lysozyme upon lyophilization. Likewise, recent hydrogen isotope-exchange/high-resolution NMR (13) and FTIR (14, 15) investigations of various proteins strongly point to lyophilization-induced reversible denaturation.

Recent advances, both instrumental and conceptual, in FTIR spectroscopy make it a method of choice for examining the structure of solid proteins. This has been illustrated by the scholarly work of Prestrelski *et al.* (14, 15), who have employed this methodology to quantify changes in the secondary structure of proteins caused by lyophilization. Using the second derivatives of the vibrational spectra of proteins in the amide

I band region ( $1600$ – $1720\text{ cm}^{-1}$ ), these authors have calculated so-called correlation coefficients which reflect the overall changes in the secondary structure upon lyophilization. This approach, however, yields no quantitative information about changes in the individual structural elements—e.g., percentages of  $\alpha$ -helices and  $\beta$ -sheets. This is because although the FTIR bands in the amide I region directly correspond to these secondary structural elements (16, 17), the line broadening in the spectra of lyophilized proteins, combined with strongly overlapping bands, make such quantitation in this region arduous (15, 18). Another spectral region, the amide III band ( $1220$ – $1330\text{ cm}^{-1}$ ), also reflects the secondary structure of proteins (19–21) and has been used to characterize structural changes qualitatively (22–26) and, in aqueous solution, even to quantify the individual secondary structure composition of proteins (19–21, 27).

We have employed the IR amide III band region to investigate quantitatively the reversible changes in the secondary structure of some dozen different proteins occurring upon lyophilization. Consequently, alterations in the individual structural elements have been determined. For all the proteins examined, lyophilization leads to a marked increase in the percentages of  $\beta$ -sheets, with a parallel drop in the percentages of  $\alpha$ -helices and unordered structures.

## MATERIALS AND METHODS

**Materials.** Bovine pancreatic trypsin inhibitor (BPTI), RNase A (90 Kunitz units/mg of protein), chymotrypsinogen A, porcine insulin ( $Zn^{2+}$  content of 0.5%), horse myoglobin (Mb) (95–100% purity), and cytochrome *c* (Cyt *c*) from the heart of tuna (98% purity), rabbit (97% purity), pigeon (99% purity), chicken (100% purity), horse (99% purity), dog (99% purity), and cow (99% purity) were obtained from Sigma. Recombinant human albumin (rHA) was a generous gift from Delta Biotechnology (Nottingham, U.K.). KBr for making pellets was from SpectraTech (Stamford, CT); acetone, propanol and D-sorbitol were from Aldrich.

**Lyophilization.** All aqueous protein solutions to be lyophilized were frozen in liquid nitrogen and applied to a Labconco (Kansas City) model 8 freeze-drier at a pressure of approximately  $10\text{ }\mu\text{m}$  of Hg and a condenser temperature of  $-50^\circ\text{C}$  for at least 24 h. Concentrations of all proteins, except for BPTI, were 10 mg/ml in distilled water unless stated otherwise. BPTI and D-sorbitol were lyophilized, separately or together, from a concentration of 1 mg/ml at pH 3.5. The pH of solutions from

Abbreviations: BPTI, bovine pancreatic trypsin inhibitor; Cyt *c*, cytochrome *c*; FTIR, Fourier-transform infrared; rHA, recombinant human albumin; Mb, myoglobin.

\*To whom reprint requests should be addressed.

which proteins were lyophilized (adjusted by adding 0.1 N NaOH or HCl) was chosen to allow comparison with spectroscopic results in the literature. For BPTI, it was pH 3.5 for comparison with results of Desai *et al.* (13). Mb was lyophilized from pH 7.0 since the crystals used for x-ray crystallography (28) were grown at this pH (29). For the same reason, pH 4.5 was chosen for chymotrypsinogen (30), pH 5.7 was chosen for RNase A (31), and pH 6.4 was chosen for horse heart Cyt c (32). All other cytochromes were studied at pH 6.4 to allow comparison with the horse heart protein. rHA was lyophilized from pH 7.3 (33); the x-ray data were obtained at neutral pH (34). Insulin was lyophilized from pH 4.0.

**Alternative Drying Methods for BPTI.** Rotary evaporation and acetone precipitation were performed as described (35). Precipitation of BPTI from aqueous solution (100 mg/ml; pH 3.5) with propanol was the same as with acetone.

**FTIR Measurements.** FTIR spectra were measured by using a Nicolet Magna-IR System 550 optical bench equipped with a MCT-B liquid-N<sub>2</sub>-cooled detector (11,700–400 cm<sup>-1</sup>), Ge beam splitter on KBr substrate (7400–350 cm<sup>-1</sup>), and a high-intensity, air-cooled mid-IR Ever-Glo source (9600–50 cm<sup>-1</sup>). The system, with a resolution specification of 0.5 cm<sup>-1</sup>, was controlled via an interface card by an analytical workstation (486DX266 Intel processor). The system was aligned by using the Nicolet OMNIC 1.2 software before the measurements and every 3 h thereafter. The data collection and calculation of second derivative spectra were carried out with the same software. The optical bench was purged with dry N<sub>2</sub> to reduce interfering water vapor IR absorption.

The solution spectra of proteins in H<sub>2</sub>O were measured using a 15-μm spacer (36) in a SpectraTech liquid cell equipped with CaF<sub>2</sub> windows. Aqueous solutions of the original proteins and of the reconstituted powders were measured at the same pH and concentration (2.5–5%). Protein powders were measured at 1 mg of protein per 200 mg of KBr. After homogenizing the lyophilized protein and KBr with an agate mortar and pestle, the powders were pressed into pellets by using a SpectraTech Macro-Micro KBr Die Kit and a Carver Laboratory (Menomonee Falls, WI) 12-ton hydraulic press. This method introduces no artifactual structural changes (14, 15). We verified that no appreciable water was absorbed during the procedure by measuring KBr pellets without protein. A total of 256 scans at 2 cm<sup>-1</sup> resolution using Happ–Genzel apodization were averaged (14, 15).

When necessary, spectra were corrected for the background in an interactive manner. Subtraction of the water background for aqueous solutions was accomplished by using the Nicolet OMNIC 1.2 software with the following goals: (i) a straight baseline in the region of 1800–2500 cm<sup>-1</sup>, where proteins do not absorb (20), and (ii) disappearance of the broad band around 800 cm<sup>-1</sup> (19). For BPTI precipitated with acetone and co-lyophilized with D-sorbitol, the subtraction was performed on dry samples. In the former case, the spectrum revealed residual acetone even after vacuum drying at 10 μm of Hg for 24 h. The typical acetone IR absorption bands were subtracted to obtain the undisturbed protein vibrational spectrum. Correction for D-sorbitol was performed on the basis of the disappearance of the D-sorbitol IR bands in the fingerprint region (37) of the spectrum. D-Sorbitol was lyophilized under conditions identical to those in its 1:1 (wt/wt) mixture with BPTI. This mixture was measured at 2.4 mg of BPTI per 200 mg of KBr and at 1.2 mg of D-sorbitol per 200 mg of KBr; the latter was used for subtraction.

Each protein sample was measured at least five times. Each spectrum was corrected for the background to obtain the protein vibrational spectra and then analyzed by second derivatization (38, 39) and Gaussian curve fitting (21, 40). The determined peak wavenumbers of the second derivative spectra, as well as those and areas of the fitted Gaussian bands, were averaged, and the standard deviations were calculated.

All spectra were analyzed by second derivatization in the amide I and III band regions for their component composition by using the OMNIC 1.2 software. Second derivative spectra were smoothed with an 11-point smoothing function (10.6 cm<sup>-1</sup>) by using this software.

Overall structural changes occurring upon protein dehydration were quantified by calculating the correlation coefficient *r* (14, 15) from the second derivative spectra in the amide I and III spectral regions. The *r* value reflects differences of two spectra: for identical ones it is 1, for those with nothing in common it is 0. The second derivative spectra used were stored as ASCII xy pair data sets (one set of data per cm<sup>-1</sup>), and the correlation coefficients were calculated by using the SIGMA PLOT program for each individual spectrum of each sample with respect to the averaged reference spectrum.

Gaussian curve fitting was performed by using the GRAMS/386 program (Galactic Industries, Salem, NH) on the original (nonsmoothed) protein vibrational spectra. The number of components and their peak positions were determined by second derivatization (38, 39) and used as starting parameters. After optimization (40), each fit was performed without fixing the peak wavenumber, full width at half maximum, or height of individual bands. Note that due to a better separation of the individual bands, the problems encountered in the analysis of the amide I region, leading to some subjectivity (18, 40), are abolished. In all cases, a linear baseline was fitted (20, 21). The secondary structural element content was calculated from the areas of the individual assigned bands and their fraction of the total area in the amide III region.

**Band Assignment in the Amide III Region.** Table 1 summarizes the results of the component analysis by second derivatization and the secondary structure quantification by Gaussian curve fitting in the amide III region for the proteins studied. In most cases, the discrepancy between the peak maxima determined by these two methods was below 3 cm<sup>-1</sup>. Larger deviations observed for some components are still in the range of published ones (21). The assignment of individual components to secondary structural elements was as follows: α-helix, 1293–1328 cm<sup>-1</sup>; β-sheet, 1225–1250 cm<sup>-1</sup>, and others, 1257–1288 cm<sup>-1</sup> (21). We independently verified every assignment by comparison with x-ray structures, as well as with secondary-structure estimates from FTIR spectra in the amide I region (17) and circular dichroism estimates (41, 42) when available.

For proteins containing significant fractions of both α-helix and β-sheet elements (BPTI, chymotrypsinogen, RNase A), the agreement between the secondary structure contents in Table 1 and the literature x-ray data is excellent. For BPTI in solution at pH 9.0, the calculated α-helix and β-sheet contents of 19% ± 2% and 40% ± 1%, respectively, were very similar to those at pH 3.5 and 7.0 (Table 2) and agree with values of 26% α-helix and 45% β-sheet derived from the x-ray studies (43–45). The FTIR-derived parameters for RNase A (23% ± 2% α-helix and 45% ± 2% β-sheet) agree with those calculated (45) from the x-ray data (23% α-helix and 45% β-sheet), as well as with other FTIR (21% α-helix and 50% β-sheet) (17) and circular dichroism data (26% α-helix and 44% β-sheet) (41). Finally, our data for chymotrypsinogen (13% α-helix and 41% β-sheet) agree with those from x-ray (11% α-helix and 46% β-sheet) (45, 46), other FTIR (21% α-helix and 50% β-sheet) (17) and circular dichroism (9% α-helix and 36% β-sheet) (42) studies.

An assignment issue has to be addressed concerning proteins with high α-helix contents (Mb, Cyt c, and rHA). FTIR studies in the amide I region have demonstrated that the extended chains connecting the α-helix cylinders absorb at frequencies similar to those of β-sheets (17). This is also the case in the amide III region at 1245 cm<sup>-1</sup> (26). We indeed observed a band at 1246 cm<sup>-1</sup> for these proteins and no

Table 1. Infrared band positions in the amide III spectral region of various proteins, band areas determined by the Gaussian curve fitting, and band assignments

Protein	Band position*				Protein	Band position*				
	Second derivative	Curve fitting	Area, %*	Assignment†		Second derivative	Curve fitting	Area, %*	Assignment†	
<b>BPTI</b>										
Solution	1317 ± 1	1316 ± 1	8 ± 1	α-Helix		1262 ± 1	1263 ± 0	11 ± 1	Unordered	
	1306 ± 2	1304 ± 1	1 ± 1	α-Helix		1240 ± 1	1247 ± 1	29 ± 1	Extended chain	
	1290 ± 1	1292 ± 1	12 ± 3	α-Helix		1221 ± 0	1227 ± 0	16 ± 1	β-Sheet	
	1282 ± 1	1277 ± 3	25 ± 6	Unordered	Horse heart Cyt c <sup>II</sup>					
	1263 ± 0	1262 ± 1	18 ± 9	Unordered	Solution	1325 ± 2	1 ± 1	α-Helix		
	1247 ± 1	1249 ± 1	6 ± 2	β-Sheet		1315 ± 0	1315 ± 1	22 ± 2	α-Helix	
Powder	1237 ± 1	1238 ± 0	30 ± 1	β-Sheet		1300 ± 1	1298 ± 1	13 ± 2	α-Helix	
	1315 ± 1	1312 ± 2	5 ± 2	α-Helix		1283 ± 2	1282 ± 0	14 ± 2	Unordered	
	1304 ± 2	‡	‡	α-Helix		1276 ± 1	1274 ± 1	1 ± 1	Unordered	
	1288 ± 0	1284 ± 1	12 ± 2	Unordered		1264 ± 1	1267 ± 1	19 ± 1	Unordered	
	1263 ± 1	1262 ± 1	28 ± 2	Unordered		1244 ± 0	1243 ± 2	27 ± 3	Extended chain	
	1246 ± 2	1246 ± 1	10 ± 2	β-Sheet	Powder	1235 ± 0	1233 ± 1	3 ± 2	β-Sheet	
	1234 ± 1	1233 ± 1	45 ± 2	β-Sheet		‡	1325 ± 2	5 ± 2	α-Helix	
RNase A							1312 ± 1	1310 ± 0	12 ± 4	α-Helix
Solution	1318 ± 0	1321 ± 0	4 ± 0	α-Helix		1303 ± 1	1298 ± 2	6 ± 1	α-Helix	
	1310 ± 2	1311 ± 0	9 ± 0	α-Helix		1284 ± 0	1284 ± 1	14 ± 3	Unordered	
	1293 ± 0	1296 ± 1	10 ± 2	α-Helix		≈1270	1272 ± 2	4 ± 2	Unordered	
	1283 ± 1	1281 ± 3	8 ± 2	Unordered		1263 ± 0	1261 ± 2	20 ± 4	Unordered	
	1264 ± 1	1261 ± 1	23 ± 3	Unordered		1244 ± 1	1249 ± 1	3 ± 2	Extended chain	
	1249 ± 0	1251 ± 1	4 ± 1	β-Sheet		1237 ± 0	1239 ± 1	23 ± 5	β-Sheet	
	1236 ± 1	1238 ± 0	42 ± 2	β-Sheet	Mb	≈1225	1225 ± 2	12 ± 2	β-Sheet	
Powder	1313 ± 0	1311 ± 0	12 ± 0	α-Helix	Solution	1319 ± 2	1322 ± 1	10 ± 3	α-Helix	
	1293 ± 1	1290 ± 1	6 ± 1	α-Helix		1314 ± 1	1308 ± 2	34 ± 3	α-Helix	
	1283 ± 1	1276 ± 2	7 ± 0	Unordered		1296 ± 1	1294 ± 1	9 ± 2	α-Helix	
	1262 ± 0	1263 ± 1	9 ± 0	Unordered		1279 ± 1	1282 ± 1	10 ± 4	Unordered	
	1245 ± 1	1253 ± 2	4 ± 3	β-Sheet		1270 ± 1	1270 ± 2	20 ± 4	Unordered	
	1233 ± 0	1236 ± 2	62 ± 3	β-Sheet		1247 ± 0	1247 ± 1	15 ± 2	Extended chain	
Chymotrypsinogen						1233 ± 2	1230 ± 2	1 ± 1	β-Sheet	
Solution	1318 ± 0	1318 ± 0	3 ± 0	α-Helix		1221 ± 0	1222 ± 1	1 ± 1	β-Sheet	
	1303 ± 0	1303 ± 1	10 ± 1	α-Helix	Powder	1311 ± 0	1312 ± 1	21 ± 0	α-Helix	
	1288 ± 1	1284 ± 0	15 ± 1	Unordered		1301 ± 1	1298 ± 0	7 ± 1	α-Helix	
	1280 ± 1	1277 ± 0	3 ± 1	Unordered		1284 ± 1	1282 ± 1	28 ± 1	Unordered	
	1266 ± 1	1265 ± 0	13 ± 1	Unordered		1261 ± 0	1259 ± 0	17 ± 1	Unordered	
	1256 ± 1	1257 ± 2	15 ± 1	Unordered		1245 ± 1	1247 ± 1	2 ± 1	Extended chain	
	1248 ± 0	1246 ± 0	15 ± 1	β-Sheet		1233 ± 2	1236 ± 1	19 ± 0	β-Sheet	
	1234 ± 0	1236 ± 1	11 ± 1	β-Sheet		1221 ± 1	1218 ± 1	6 ± 1	β-Sheet	
	‡	1228 ± 1	15 ± 2	β-Sheet	Zn-insulin					
Powder	1312 ± 0	1308 ± 1	8 ± 0	α-Helix	Solution	1334 ± 2	1332 ± 2	7 ± 2	α-Helix	
	1283 ± 1	1282 ± 0	11 ± 0	Unordered		1322 ± 1	1322 ± 2	3 ± 3	α-Helix	
	1262 ± 1	1260 ± 0	23 ± 0	Unordered		1313 ± 1	1313 ± 1	8 ± 4	α-Helix	
	1247 ± 1	1247 ± 1	3 ± 1	β-Sheet		1301 ± 1	1299 ± 2	13 ± 2	α-Helix	
	1232 ± 1	1233 ± 0	55 ± 0	β-Sheet		1287 ± 1	1285 ± 2	15 ± 3	Unordered	
rHA						1275 ± 1	1275 ± 0	3 ± 3	Unordered	
Solution	1320 ± 0	1316 ± 1	30 ± 1	α-Helix		1265 ± 1	1265 ± 0	18 ± 5	Unordered	
	1303 ± 0	1302 ± 1	1 ± 0	α-Helix		1248 ± 0	1249 ± 1	17 ± 2	β-Sheet	
	1293 ± 0	1295 ± 1	27 ± 4	α-Helix	Powder	1235 ± 1	1237 ± 1	15 ± 3	β-Sheet	
	1281 ± 1	1276 ± 1	15 ± 3	Unordered		≈1330	1327 ± 2	4 ± 2	α-Helix	
	1266 ± 2	1264 ± 0	4 ± 1	Unordered		1313 ± 0	1312 ± 1	8 ± 1	α-Helix	
	1244 ± 1	1246 ± 1	23 ± 1	Extended chain		1299 ± 1	1294 ± 1	11 ± 1	α-Helix	
	1227 ± 1	1226 ± 2	<1%	β-Sheet		1287 ± 0	1281 ± 1	9 ± 0	Unordered	
Powder	1312 ± 0	1310 ± 0	23 ± 1	α-Helix		‡	1274 ± 1	3 ± 1	Unordered	
	1302 ± 1	1294 ± 1	7 ± 0	α-Helix		1263 ± 1	1265 ± 1	13 ± 3	Unordered	
	1287 ± 1	1282 ± 1	10 ± 1	Unordered		1241 ± 1	1251 ± 2	25 ± 7	β-Sheet	
	1277 ± 1	1274 ± 1	4 ± 1	Unordered		1230 ± 0	1232 ± 4	27 ± 2	β-Sheet	

\*The ± values are the standard deviations calculated by analyzing three to five individual spectra in each case.

†Unordered structures include turns and random coils. For α-helical proteins, the extended chain secondary structure is given individually to allow comparison with FTIR results obtained in the amide I spectral region (17).

‡This component, visible as a shoulder in the second derivative spectra (see Fig. 1D), was not amenable to the Gaussian curve fitting (see Fig. 2B) because of its weakness in the original spectra.

§These components were not visible in the second derivative spectra. Nevertheless, the Gaussian curve fitting without them resulted in systematic discrepancies between the original spectra and the sums of the fitted bands. The components therefore had to be used.

¶Very similar parameters were obtained for tuna heart Cyt c (data not shown).

Table 2. Correlation coefficients and secondary structure contents for BPTI under different conditions

Protein sample	Correlation coefficient*	Secondary structure, %		
		$\alpha$ -Helix	$\beta$ -Sheet	Unordered†
<b>Aqueous solution‡</b>				
pH 3.5	1.0	21 ± 2	36 ± 2	43 ± 3
pH 7.0	1.0	20 ± 2	43 ± 1	37 ± 3
pH 9.0	0.99	19 ± 2	40 ± 1	41 ± 3
<b>Powders§</b>				
Lyophilization	0.70	5 ± 2	55 ± 0	40 ± 2
Co-lyophilization with sorbitol	1	13 ± 2	41 ± 2	46 ± 1
Precipitation with acetone	1	2 ± 1	63 ± 4	35 ± 4
Precipitation with propanol	0.51	4 ± 1	59 ± 1	37 ± 1
Rotary evaporation	0.46	1 ± 1	72 ± 2	27 ± 1
<b>Redissolved powder  </b>				
Lyophilization	0.99	20 ± 4	42 ± 2	38 ± 4
Co-lyophilization with sorbitol	0.97	23 ± 2	42 ± 1	35 ± 3
Precipitation with acetone	0.96	21 ± 3	40 ± 2	39 ± 4
Precipitation with propanol	0.98	20 ± 3	40 ± 2	40 ± 4
Rotary evaporation	0.99	25 ± 1	40 ± 2	35 ± 4

\*All standard deviations for the correlation coefficients are below 2%. All correlation coefficients are calculated (14, 15) for the amide III region vs. the aqueous solution at pH 3.5.

†Unordered structures include turns and random coil secondary structural elements.

‡Solutions of BPTI in water.

§All powders were obtained from aqueous solution at pH 3.5.

||The correlation coefficients of these samples could not be calculated. However, residual acetone and sorbitol in the pellets could be subtracted sufficiently to allow for the Gaussian curve fitting.

||For reconstitution, all dehydrated powders were redissolved in water and measured at pH 3.5 at the same concentration as the reference solutions.

significant bands at 1225–1240  $\text{cm}^{-1}$  (Table 1) typical for proteins containing  $\beta$ -sheets (21). Since circular dichroism studies indicate very low  $\beta$ -sheet contents for Cyt c and Mb (41), the 1246  $\text{cm}^{-1}$  band in these proteins was assigned to the extended chain secondary structures and bands at 1225–1240  $\text{cm}^{-1}$  to  $\beta$ -sheet structural elements. For horse heart Cyt c, the calculated  $\alpha$ -helix content (36% ± 1%) agrees with those derived from both x-ray data (36%) (32) and recent FTIR work using Gaussian curve fitting of the amide I band (36%) (47). Our calculated  $\beta$ -sheet content for this Cyt c (3%; Table 3) also

agrees with the x-ray (32) and circular dichroism data (41). The secondary structure compositions of oxidized horse and tuna heart Cyt c elucidated by our FTIR analysis coincide with those from the x-ray analysis (32, 48). For Mb, our calculated  $\alpha$ -helix content (53% ± 2%) is significantly below that estimated from the x-ray structure (80%) (28), although our calculated  $\beta$ -sheet content (2%) agrees with the x-ray and circular dichroism data (41). The secondary structure calculated for rHA (58% ± 4%  $\alpha$ -helix; 23% ± 1% extended chain) resembled x-ray estimates (67%  $\alpha$ -helix; 33% turns and extended chain) (34).

Table 3. Secondary structure contents of various proteins

Protein*	State†	Secondary structure, %		
		$\alpha$ -Helix	$\beta$ -Sheet	Unordered‡
BPTI	Solution	21 ± 2	36 ± 2	43 ± 3
	Powder	5 ± 2	55 ± 0	40 ± 2
rHA	Solution	58 ± 4	0	42 ± 3
	Powder	30 ± 1	16 ± 1	54 ± 2
Mb	Solution	53 ± 2	2 ± 1	45 ± 2
	Powder	28 ± 1	25 ± 1	47 ± 2
Horse heart Cyt c	Solution	36 ± 1	3 ± 2	61 ± 5
	Powder	23 ± 3	35 ± 2	42 ± 3
Tuna heart Cyt c	Solution	34 ± 2	2 ± 1	64 ± 2
	Powder	19 ± 2	34 ± 3	47 ± 2
RNase A	Solution	23 ± 2	45 ± 2	32 ± 2
	Powder	18 ± 1	66 ± 1	16 ± 1
Chymotrypsinogen	Solution	13 ± 1	41 ± 1	46 ± 1
	Powder	8 ± 0	58 ± 1	34 ± 0
Zn-insulin	Solution	30 ± 3	32 ± 4	38 ± 2
	Powder	23 ± 1	52 ± 5	25 ± 4

The secondary structures of proteins, both as an aqueous solution and as lyophilized powder, were calculated from Gaussian curve fitting in the amide III band region.

\*For a discussion of the secondary structures calculated in this work compared with those from x-ray studies and other spectroscopic techniques, see *Materials and Methods*.

†The pH values of the protein aqueous solutions were as follows: 3.5 for BPTI, 7.3 for rHA, 7.0 for Mb, 6.4 for both horse and tuna Cyt c, 5.7 for RNase A, 4.5 for chymotrypsinogen, and 4.0 for Zn-insulin. The protein powders were obtained by lyophilizing these aqueous solutions.

‡Unordered structures include turns, random coil, and extended chain secondary structural elements.

Our characterization of insulin yielded significantly lower  $\alpha$ -helix and higher  $\beta$ -sheet contents (30% and 32%, respectively) than the x-ray structure (53%  $\alpha$ -helix and 13%  $\beta$ -sheet) (45, 49). This may be due to differences in the pH used in our study and that for which the x-ray structure was determined (pH 6.6).

The same assignments used for the solutions were employed for the corresponding protein powders. Most spectra of dehydrated proteins were simpler than those in aqueous solutions due to band broadening and disappearance of small bands (Table 1). Upon dehydration, some FTIR bands in the amide III region undergo small shifts, as also observed for the amide I region (14, 15). Despite the observed band broadening in dehydrated protein powders, the separation of individual bands is still sufficient for proper Gaussian curve fitting by using the original vibrational spectra without resolution enhancement [required for the amide I quantification (18)].

## RESULTS AND DISCUSSION

Our recent hydrogen isotope-exchange/high-resolution NMR work (13) has unequivocally established that BPTI undergoes significant reversible structural changes upon dehydration. However, the nature of these changes could not be quantified. Consequently, herein we employed an independent methodology, FTIR spectroscopy, to address this issue in the same system. FTIR spectroscopy is one of very few methods that

allow for the quantification of protein secondary structural elements in both the amorphous and solution states.

Initially, to confirm the perturbations in BPTI structure upon lyophilization, we compared the IR spectrum of the solid protein with that in aqueous solution by using the second derivative spectra in the amide I and III regions (Fig. 1). This was accomplished by calculating the correlation coefficient  $r$  (14, 15) for the spectrum of lyophilized BPTI by using that in solution as a reference (see *Materials and Methods* for details). The calculated values of  $r = 0.70$  for the amide III region (Table 2) and  $r = 0.73$  for the amide I region were very similar, thereby validating the use of the former spectral region.

To appreciate the significance of a difference of some 0.3 in the  $r$  values, we measured solution IR spectra of BPTI at two additional pH values, 7.0 and 9.0, and calculated the correlation coefficients vs. the solution at pH 3.5. The correlation coefficients for the amide III and amide I regions, 1.0 and 0.99 (Table 2) and 0.96 and 0.96 for pH 7.0 and 9.0, respectively, are very close to unity, suggesting no appreciable structural changes, despite the 5.5-pH-unit variation. Hence, we conclude that  $r$  is not highly sensitive to structural alterations, since changes in the ionization state of ionogenic groups, which cause spectral differences (50) and undoubtedly at least small conformational perturbations, are not reflected in the calculated numbers. Therefore, the  $r$  values obtained for lyophilized BPTI, 0.70 in the amide III region, must represent rather drastic changes in the secondary structure. Thus, our analysis

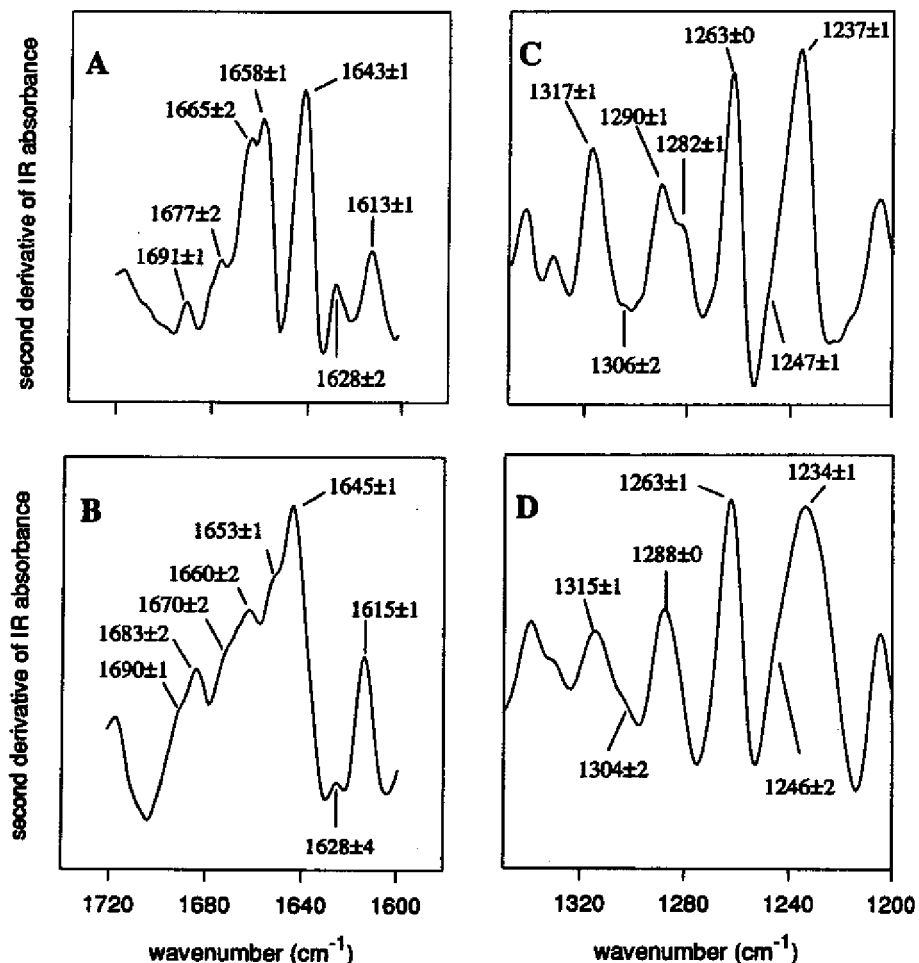


FIG. 1. Second derivative FTIR spectra (multiplied by -1) of BPTI in aqueous solution at pH 3.5 (A and C) and in the powder obtained by lyophilization from that solution (B and D). The wavenumbers shown are the average values for the peaks and shoulders from five independent spectra. A and B depict the amide I region, and C and D depict the amide III spectral region.

of both spectral regions indicates that BPTI undergoes a significant lyophilization-induced structural rearrangement.

Inspection of the second derivative spectra (Fig. 1) reveals additional structural information not evident from the correlation coefficients. In the BPTI solution spectrum in the amide I region (Fig. 1A), two major bands at  $1658$  and  $1643\text{ cm}^{-1}$  are clearly visible. The former with a shoulder at  $1665\text{ cm}^{-1}$  can be assigned to  $\alpha$ -helix and random coil secondary structural elements, respectively, whereas the latter arises from the  $\beta$ -sheet (16, 51). BPTI lyophilized powder (Fig. 1B) has only one major band in this spectral region at  $1645\text{ cm}^{-1}$ . The second derivative spectrum of the aqueous solution of BPTI in the amide III region (Fig. 1C) shows several well-resolved bands, which were assigned to the secondary structural elements according to Fu *et al.* (21) (Table 1). The major spectral change upon lyophilization (Fig. 1D) is a significant broadening (the full width at half maximum increased from  $13 \pm 1$  to  $28 \pm 2\text{ cm}^{-1}$ ) of the band at  $1237\text{ cm}^{-1}$  assigned to the  $\beta$ -sheet structural element. Comparison of Fig. 1B and D demonstrates the superior band separation in the amide III region in the solid state compared with that in the amide I region.

Inspection of the original spectra in the amide III region qualitatively confirms the pronounced structural changes upon lyophilization (Fig. 2). The spectrum of lyophilized BPTI is dominated by a band at  $1238\text{ cm}^{-1}$  (Fig. 2B). The bands originating from  $\alpha$ -helix and unordered secondary structural elements ( $1320$ – $1263\text{ cm}^{-1}$ ), clearly visible in the solution spectrum (Fig. 2A), appear only as shoulders in the lyophilized powder spectrum (Fig. 2B). This indicates a conversion from  $\alpha$ -helix/unordered structure to  $\beta$ -sheet structural elements.

Comparison of the original and second derivative spectra and the calculation of correlation coefficients, while instructive, yield no quantitative information about variations in the  $\alpha$ -helix and  $\beta$ -sheet contents. To quantify the structural changes occurring upon lyophilization of BPTI, we performed Gaussian curve fitting of the IR spectra in the amide III region (Fig. 2). The results (Table 2) reveal a drop in the  $\alpha$ -helix content from 21% to 5% and a rise in the  $\beta$ -sheet content from 36% to 55% upon lyophilization. These data provide a quantitative confirmation of the previous qualitative observations (13).

Desai *et al.* (13) further demonstrated that co-lyophilization with the lyoprotectant sorbitol lowered the magnitude of

BPTI's structural rearrangement. We found (Table 2) that BPTI co-lyophilized with sorbitol has a secondary structure similar to that observed in solution. In particular, the  $\beta$ -sheet content is essentially the same, indicating that the protein core [which consists mainly of antiparallel  $\beta$ -sheets (43, 44)] is conserved. Note, however, that the content of  $\alpha$ -helices in BPTI, located on the periphery of the molecule (43, 44), is not fully conserved. The 13%  $\alpha$ -helix content of BPTI in the co-lyophilizate with sorbitol is between that of the lyophilized powder (5%) and that in aqueous solution (21%). The calculated correlation coefficients (for amide I region) also reflect this partial structural preservation: 0.84 for the co-lyophilizate vs. 0.73 for BPTI lyophilized in the absence of sorbitol.

To distinguish whether the observed structural changes in BPTI are caused by the dehydration of the protein *per se* or are specific to lyophilization, we explored alternative drying methods: precipitation with acetone or propanol and rotary evaporation. When compared with the lyophilized powder, the resultant dried samples yielded correlation coefficients (Table 2) indicative of larger structural changes. This is also seen in the secondary structural compositions (Table 2). In particular, in the case of rotary evaporation, there is nearly twice as large an increase in the  $\beta$ -sheet content when compared with lyophilization, and most of this rise comes from the drop in the unordered structure content. These findings are consistent with those obtained by hydrogen isotope exchange/NMR (35), which demonstrated the superiority of lyophilization in conserving BPTI's native structure compared with the alternative dehydration methods.

Having established that BPTI's secondary structure undergoes major rearrangements upon dehydration, an important question was whether this phenomenon is reversible. To answer it, all dehydrated BPTI samples were redissolved in water (pH 3.5), and their IR solution spectra were determined. The  $r$  values for these solutions vs. the protein solution prior to dehydration, as well as the secondary structure contents, show unequivocally (Table 2) that all dehydration-induced structural changes were fully reversible.

Our BPTI data reveal that the  $\alpha$ -helix content decreases and the  $\beta$ -sheet content increases upon dehydration. It was important to establish whether this is a general phenomenon. To this end, we lyophilized 12 different proteins and quantified their secondary structural compositions from the IR spectra.

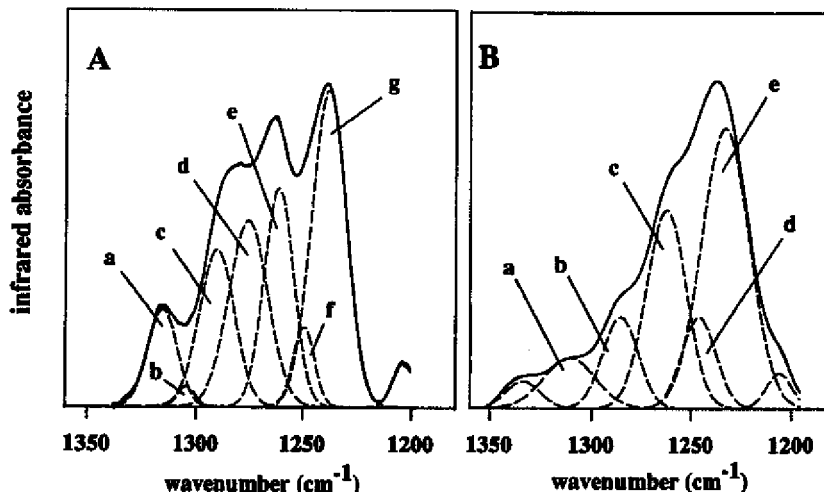


FIG. 2. FTIR spectra of BPTI in aqueous solution at pH 3.5 (A) and the powder lyophilized from that solution (B) after the Gaussian curve-fitting process. The results of the added Gaussian bands and the original spectra (solid lines) are superimposed and are nearly identical. The area of the individual Gaussian bands (broken lines) has been used to calculate the secondary structure content. The individual bands were assigned as follows: (A) a, b, and c,  $\alpha$ -helix; d and e, unordered; f and g,  $\beta$ -sheet; (B) a,  $\alpha$ -helix; b and c, unordered; d and e,  $\beta$ -sheet. The bands at  $\sim 1205\text{ cm}^{-1}$  are not an amide III vibration (21) and are presented solely for the fit. The band at around  $1340\text{ cm}^{-1}$  in the spectrum of the powder (B), which is of an unknown origin and not found in the BPTI spectrum in aqueous solution, was not assigned to any secondary structural element.

Among the proteins studied, there were seven forms of Cyt c (from dog, rabbit, pigeon, chicken, bovine, horse, and tuna hearts). Despite some differences in their primary structures, the IR spectra for the cytochromes were virtually identical both in solution and in the lyophilized states. The correlation coefficients calculated for the Cyt c solutions vs. the one for the horse heart Cyt c solution (pH 6.4) in the amide III region were all  $>0.93$  with the exception of tuna Cyt c ( $r = 0.87$ ). Moreover, the correlation coefficients for the spectra of all lyophilized Cyt cs vs. the one for lyophilized horse Cyt c were all  $\geq 0.97$ . Therefore, hereafter we consider only the FTIR data for the two most dissimilar cytochromes, those from horse and tuna hearts.

Table 3 summarizes the secondary structures calculated for eight proteins in solution and in the lyophilized state. [We also quantified the secondary structural elements of the proteins following their reconstitution in water (data not shown) and established that all structural changes caused by lyophilization were reversible.] It is seen that all the proteins studied exhibited pronounced secondary structural changes upon lyophilization: in every case, the  $\alpha$ -helical content decreased and the  $\beta$ -sheet content increased significantly, although the magnitude of this effect varied among the proteins.

Of the proteins studied, rHA exhibited the largest decrease in  $\alpha$ -helical content upon lyophilization, from 58% to 30%. Its  $\beta$ -sheet content rose from 0% to 16%, and the unordered secondary structure rose from 42% to 54%. It is noteworthy that rHA is the only protein in our study to exhibit an increase in unordered structure, indicating that this protein partially unfolds upon lyophilization.

The data for Mb show a precipitous drop in the  $\alpha$ -helix content and a parallel increase in the  $\beta$ -sheet content, while the fraction of unordered structures remains the same. For both cytochromes, significant decreases in the  $\alpha$ -helical content and  $\sim 10$ -fold increases in  $\beta$ -sheet content occurred upon dehydration. The unordered structure of both cytochromes decreased substantially, suggesting a higher structural order in the lyophilized state. For RNase A, chymotrypsinogen, and insulin, only minor decreases in the  $\alpha$ -helix content but substantial increases in the  $\beta$ -sheet content took place upon lyophilization. For lyophilized insulin, these dehydration-induced structural changes are in line with recent Raman spectroscopy findings comparing bovine Zn-insulin powders with those dissolved in aqueous solutions (52). Note that for all three proteins the percentage of the unordered structures drops upon lyophilization indicating an overall increase in the structural order.

For every protein studied, even those belonging to different structural classes (17), we observed a decrease in  $\alpha$ -helices and a concomitant increase in  $\beta$ -sheets upon lyophilization (Fig. 3). Similar behavior was reported for poly(L-lysine) (15), where, regardless of the secondary structure in aqueous solution, the lyophilized polypeptide mainly consisted of  $\beta$ -sheets. It has been predicted that dehydration should induce major structural changes in proteins (53). For instance, Barlow and Poole (54) demonstrated that water molecules hydrogen bond to the C=O groups of the peptide backbone in  $\alpha$ -helical but not  $\beta$ -sheet regions; therefore, dehydration should disrupt the former but not the latter portions of the protein molecule. The most likely reason for a marked increase in the  $\beta$ -sheet content of the proteins upon dehydration appears to be formation of intermolecular  $\beta$ -sheet structures, which are entropically prohibitive in solution. In the solid—e.g., lyophilized form—where protein molecules are forced into contact with each other and there is no competing bulk water molecules, such intermolecular interactions presumably become energetically attractive.

The secondary structural transitions depicted in Fig. 3 have also been reported for adsorption of proteins to surfaces. The adsorption of human serum albumin to polymeric contact lens

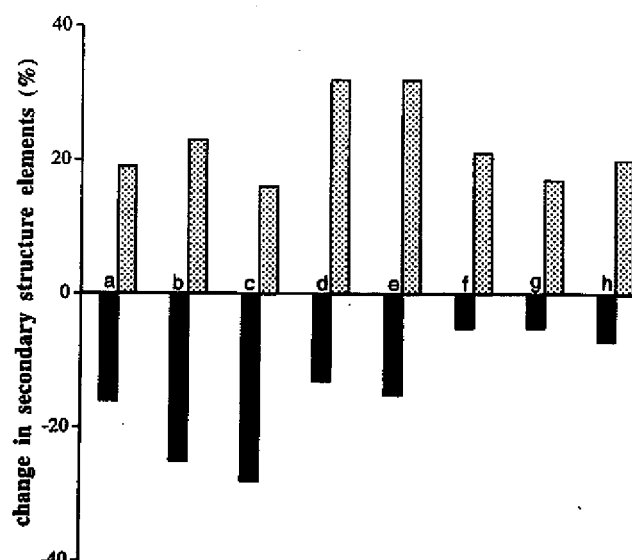


FIG. 3. Changes in the  $\alpha$ -helix (solid bars) and  $\beta$ -sheet (dotted bars) content upon lyophilization, as determined by the Gaussian curve fitting of the FTIR spectra of aqueous solutions and lyophilized powders for the following proteins: a, BPTI; b, Mb; c, rHA; d, horse heart Cyt c; e, tuna heart Cyt c; f, RNase A; g, chymotrypsinogen, and h, insulin.

material is accompanied by a conversion of  $\alpha$ -helices and random coils to  $\beta$ -sheets (55). Under these conditions, lysozyme undergoes an  $\alpha$ -helix to  $\beta$ -sheet conversion (56) and mucin undergoes a random coil to  $\beta$ -sheet conversion (57). Another example is the adsorption of fibronectin to polyurethane surfaces, which induces a random coil to  $\beta$ -sheet conversion (24).

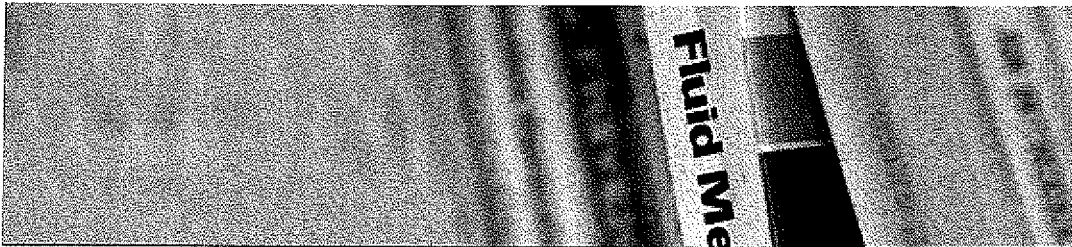
More closely related to the dehydration-induced structural changes reported herein are those accompanying protein aggregation, another process resulting in increased protein-protein contacts. Thermal aggregation raises the  $\beta$ -sheet content in acetylcholinesterase (58) and ovalbumin (59). Precipitation with salt increases the  $\beta$ -sheet content and decreases the  $\alpha$ -helix content of proteins (60). Aggregation of the M13 coat protein (61) and inclusion-body formation of  $\beta$ -lactamase (62) also increase  $\beta$ -sheet content. Finally, an  $\alpha$ -helix to  $\beta$ -sheet conversion parallels the solubility decrease in insulinotropin (63).

In summary, by means of FTIR spectroscopy, we found that upon dehydration proteins undergo a marked reversible change in secondary structure: the  $\beta$ -sheet content goes up while the  $\alpha$ -helix content goes down. For almost all the proteins studied, lyophilization makes the protein structure more ordered by decreasing the percentage of unordered structures. These structural changes must be considered in analyzing the behavior of dry proteins.

We thank Profs. Robert Langer and Jonathan King and Dr. Henry R. Costantino for helpful discussions. We also thank Dr. Henry R. Costantino for preparing rHA for FTIR measurements. This work was funded by National Institutes of Health Grant GM26698 and the Biotechnology Process Engineering Center at the Massachusetts Institute of Technology.

1. Costantino, H. R., Langer, R. & Klibanov, A. M. (1994) *J. Pharm. Sci.* **83**, 1662–1669.
2. Klibanov, A. M. (1990) *Acc. Chem. Res.* **23**, 114–120.
3. Careri, G., Giansanti, A. & Gratton, E. (1979) *Biopolymers* **18**, 1187–1203.
4. Careri, G., Gratton, E., Yang, P.-H. & Rupley, J. A. (1980) *Nature (London)* **284**, 572–573.
5. Rupley, J. A., Gratton, E. & Careri, G. (1983) *Trends Biochem. Sci.* **8**, 18–22.

6. Rupley, J. A. & Careri, G. (1991) *Adv. Protein Chem.* **41**, 37–172.
7. Schinkel, J. E., Downer, N. W. & Rupley, J. A. (1985) *Biochemistry* **24**, 352–366.
8. Baker, L. J., Hansen, A. M. F., Rao, P. B. & Bryan, W. P. (1983) *Biopolymers* **22**, 1637–1640.
9. Yu, N.-T. & Jo, B. H. (1973) *Arch. Biochem. Biophys.* **156**, 469–474.
10. Poole, P. L. & Finney, J. L. (1983) *Int. J. Biol. Macromol.* **5**, 308–310.
11. Poole, P. L. & Finney, J. L. (1983) *Biopolymers* **22**, 255–260.
12. Gregory, R. B., Gangoda, M., Gilpin, R. K. & Su, W. (1993) *Biopolymers* **33**, 513–519.
13. Desai, U. R., Osterhout, J. J. & Klibanov, A. M. (1994) *J. Am. Chem. Soc.* **116**, 9420–9422.
14. Prestrelski, S. J., Arakawa, T. & Carpenter, J. F. (1993) *Arch. Biochem. Biophys.* **303**, 465–473.
15. Prestrelski, S. J., Tedischi, N., Arakawa, T. & Carpenter, J. F. (1993) *Biophys. J.* **65**, 661–671.
16. Surewicz, W. K. & Mantsch, H. H. (1988) *Biochim. Biophys. Acta* **952**, 115–130.
17. Byler, D. M. & Susi, H. (1986) *Biopolymers* **25**, 469–487.
18. Dong, A., Prestrelski, S. J., Allison, D. & Carpenter, J. F. (1995) *J. Pharm. Sci.* **84**, 415–424.
19. Singh, B. R., Fuller, M. P. & Schiavo, G. (1990) *Biophys. Chem.* **46**, 155–166.
20. Singh, B. R., DeOliveira, D. B., Fu, F.-N. & Fuller, M. P. (1993) *SPIE 1890* (Biomol. Spectr. III), 47–55.
21. Fu, F.-N., DeOliveira, D. B., Trumple, W. R., Sakar, H. K. & Singh, B. R. (1994) *Appl. Spectrosc.* **48**, 1432–1441.
22. Kaiden, K., Matsui, T. & Tanaka, S. (1987) *Appl. Spectrosc.* **41**, 180–184.
23. Kato, K., Matsui, T. & Tanaka, S. (1987) *Appl. Spectrosc.* **41**, 861–865.
24. Pitt, W. G., Spiegelberg, S. H. & Cooper, S. L. (1987) in *Proteins at Interfaces*, eds. Brush, J. L. & Horbett, T. A. (Am. Chem. Soc., Washington, DC), pp. 324–338.
25. Wasacz, F. M., Ohlinger, J. M. & Jakobsen, R. J. (1987) *Biochemistry* **26**, 1464–1470.
26. Jakobsen, R. J. & Wasacz, F. M. (1987) in *Proteins at Interfaces*, eds. Brush, J. L. & Horbett, T. A. (Am. Chem. Soc., Washington, DC), pp. 339–361.
27. Singh, B. R., Fu, F.-N. & Ledoux, D. N. (1994) *Struct. Biol.* **1**, 358–360.
28. Evans, S. V. & Brayer, G. D. (1990) *J. Mol. Biol.* **213**, 885–897.
29. Sherwood, C., Mauk, A. G. & Brayer, G. D. (1987) *J. Mol. Biol.* **193**, 227.
30. Wang, D., Bode, W. & Huber, R. (1985) *J. Mol. Biol.* **185**, 595–624.
31. Carlisle, C. H., Palmer, R. A., Mazumdar, S. K., Gorinsky, B. A. & Yeates, D. G. (1974) *J. Mol. Biol.* **85**, 1–18.
32. Bushnell, G. W., Louie, G. V. & Brayer, G. D. (1990) *J. Mol. Biol.* **214**, 585–595.
33. Costantino, H. R., Langer, R. & Klibanov, A. M. (1995) *Bio/Technology* **13**, 493–496.
34. He, X. M. & Carter, D. C. (1992) *Nature (London)* **358**, 209–215.
35. Desai, U. R. & Klibanov, A. M. (1995) *J. Am. Chem. Soc.* **117**, 3940–3945.
36. Singh, B. R. & Fuller, M. P. (1991) *Appl. Spectrosc.* **45**, 1017–1021.
37. Carpenter, J. F. & Crowe, J. H. (1989) *Biochemistry* **28**, 3916–3922.
38. Susi, H. & Byler, D. M. (1983) *Biochem. Biophys. Res. Commun.* **115**, 391–397.
39. Susi, H. & Byler, D. M. (1986) *Methods Enzymol.* **130**, 291–311.
40. Abbott, T. F., Wolf, W. J., Wu, Y. V., Butterfield, R. O. & Kleiman, R. (1991) *Appl. Spectrosc.* **45**, 1665–1673.
41. Provencher, S. W. & Glöckner, J. (1981) *Biochemistry* **20**, 33–37.
42. Chen, Y.-H., Yang, J. T. & Martinez, H. M. (1972) *Biochemistry* **11**, 4120–4131.
43. Huber, R., Kukla, D., Rühlmann, A., Epp, O. & Formanek, H. (1970) *Naturwissenschaften* **57**, 389–392.
44. Deisenhofer, J. & Steigemann, W. (1975) *Acta Crystallogr. B* **31**, 238–250.
45. Levitt, M. & Greer, J. (1977) *J. Mol. Biol.* **114**, 181–293.
46. Freer, S. T., Kraut, J., Robertus, J. D., Wright, H. T. & Xuong, N. H. (1970) *Biochemistry* **9**, 1997–2009.
47. Heimburg, T. & Marsh, D. (1993) *Biophys. J.* **65**, 2408–2417.
48. Takano, T. & Dickerson, R. E. (1981) *J. Mol. Biol.* **153**, 95–115.
49. Blundell, T. L., Dodson, G., Hodkin, D. & Mercola, D. (1972) *Adv. Protein Chem.* **26**, 279–402.
50. Venyaminov, S. Y. & Kalinin, N. N. (1990) *Biopolymers* **30**, 1243–1257.
51. Ohlinger, J. M., Hill, D. M., Jakobsen, R. J. & Brody, R. S. (1986) *Biochim. Biophys. Acta* **869**, 89–98.
52. Yeo, S.-D., DeBenedetti, P. G., Patro, S. Y. & Przybycien, T. M. (1994) *J. Pharm. Sci.* **83**, 1651–1656.
53. Kuntz, I. D., Jr., & Kauzmann, W. (1974) *Adv. Protein Chem.* **28**, 239–345.
54. Barlow, D. J. & Poole, P. L. (1987) *FEBS Lett.* **213**, 423–427.
55. Castillo, E. J., Koenig, J. L., Anderson, J. M. & Lo, J. (1984) *Biomaterials* **5**, 319–325.
56. Castillo, E. J., Koenig, J. L., Anderson, J. M. & Lo, J. (1985) *Biomaterials* **6**, 338–345.
57. Castillo, E. J., Koenig, J. L., Anderson, J. M. & Jentoft, N. (1986) *Biomaterials* **7**, 9–15.
58. Görne-Tschelnokow, U., Naumann, D., Weise, C. & Hucho, F. (1993) *Eur. J. Biochem.* **213**, 1235–1242.
59. Kato, A. & Takagi, T. J. (1988) *Agric. Food Chem.* **36**, 1156–1159.
60. Przybycien, T. M. & Bailey, J. E. (1989) *Biochim. Biophys. Acta* **995**, 231–245.
61. Spruijt, R. B., Wolfs, C. J. A. & Hemminga, M. A. (1989) *Biochemistry* **28**, 9158–9165.
62. Przybycien, T. M., Dun, J. P., Valax, P. & Georgiou, G. (1994) *Protein Eng.* **7**, 131–136.
63. Kim, Y., Rose, C. A., Liu, Y., Ozaki, Y., Datta, G. & Tu, A. T. (1994) *J. Pharm. Sci.* **83**, 1175–1180.

**Titre du document / Document title**

Relationship between conformational stability and lyophilization-induced structural changes in chymotrypsin

**Auteur(s) / Author(s)**

CARRASQUILLO K. G. (1) ; SANCHEZ C. (1) ; GRIEBENOW K. (1) ;

**Affiliation(s) du ou des auteurs / Author(s) Affiliation(s)**

(1) Department of Chemistry, University of Puerto Rico, Rio Piedras Campus, P.O. Box 23346, San Juan, PR 00931-3346, PORTO RICO

**Résumé / Abstract**

The relationship between protein conformational stability in aqueous solution and the magnitude of lyophilization-induced structural changes was investigated employing  $\alpha$ - and  $\gamma$ -chymotrypsin. As a measure of the conformational stability the melting temperature  $T_m$  was determined in distilled water at various pH values. The proteins were then lyophilized from those pH values where the conformational stability was maximum (pH 4.5) and minimum (pH 7.8). Protein secondary structure was quantitatively determined utilizing Fourier-transform infrared spectroscopy employing two regions sensitive to protein structure, the amide-I ( $1600$ - $1700$   $\text{cm}^{-1}$ ) and amide-III ( $1215$ - $1335$   $\text{cm}^{-1}$ ). Lyophilization induced significant structural alterations in both proteins, characterized by a slight decrease in the  $\alpha$ -helix and a significant increase in the  $\beta$ -sheet content. However, regardless of the pH from which the proteins were lyophilized, the secondary structures in the solid state were indistinguishable. This result shows that there is no relationship between the conformational stability in aqueous solution and the magnitude of lyophilization-induced structural changes. We also investigated whether lyoprotectants could minimize lyophilization-induced structural changes by increasing protein conformational stability in aqueous solution. After having identified trehalose as being efficient in largely preventing lyophilization-induced structural alterations, we conducted co-lyophilization experiments from various pH values. The results obtained exclude any contribution from increased protein conformational stability caused by the additive in aqueous solution to the beneficial structural preservation upon lyophilization. This can be understood because the dehydration and not the freezing process, as shown in an air-drying experiment, mainly causes protein structural alterations.

**Revue / Journal Title**

Biotechnology and applied biochemistry ISSN 0885-4513 CODEN BABIEC

**Source / Source**

2000, vol. 31, n°1, pp. 41-53 (59 ref.)

**Langue / Language**

Anglais

**Editeur / Publisher**

Portland Press, London, ROYAUME-UNI (1986) (Revue)

**Mots-clés anglais / English Keywords**

Chymotrypsin ; Stability ; Freeze drying ; Alteration ; Secondary structure ; Industrial application ; Pharmaceutical industry ; Formulation ; Conformation ; Serine endopeptidases ; Peptidases ; Hydrolases ; Enzyme ;

**Mots-clés français / French Keywords**

Chymotrypsin ; Stabilité ; Lyophilisation ; Altération ; Structure secondaire ; Application industrielle ; Industrie pharmaceutique ; Formulation ; Conformation ; Serine endopeptidases ; Peptidases ; Hydrolases ; Enzyme ;

**Mots-clés espagnols / Spanish Keywords**

Chymotrypsin ; Estabilidad ; Liofilización ; Alteración ; Estructura secundaria ; Aplicación industrial ; Industria farmacéutica ; Formulación ; Conformación ; Serine endopeptidases ; Peptidases ; Hydrolases ; Enzima ;

**Localisation / Location**

INIST-CNRS, Cote INIST : 17979, 35400008663446.0060

**Copyright 2008 INIST-CNRS. All rights reserved**

Toute reproduction ou diffusion même partielle, par quelque procédé ou sur tout support que ce soit, ne pourra être faite sans l'accord préalable écrit de l'INIST-CNRS.

No part of these records may be reproduced or distributed, in any form or by any means, without the prior written  
permission of INIST-CNRS.

N° notice refdoc (ud4) : 1283499

[Rechercher dans CAT.INIST / Search in CAT.INIST](#)

 Google Custom Search